Scientific
Research
Publishing

Spatio-Temporal Agricultural Drought Quantification in a Rainfed Agriculture, Athi-Galana-Sabaki River Basin

Joe Ndundi Tete[1,2]*, Godfrey Ouma Makokha[1] , Oscar Owino Ngesa[1], John Ngugi Muthami[1], Bonface Wabwire Odhiambo[1]

[1]Department of Informatics and Computing, Taita Taveta University, Voi, Kenya
[2]Department of Finance and Economic Planning, County Government of Kilifi, Kilifi, Kenya
Email: *joendunditete@gmail.com, makokha.godfrey@ttu.ac.ke, oscanges@ttu.ac.ke, johnngugi0407@gmail.com, bonfaceodhiambo291@gmail.com

Abstract

This study employs a quantitative approach to comprehensively investigate the full propagation process of agricultural drought, focusing on pigeon peas (the most grown crop in the AGS Basin) planting seasonal variations. The study modelled seasonal variabilities in the seasonal Standardized Precipitation Index (SPI) and Standardized Agricultural Drought Index (SADI). To necessitate comparison, SADI and SPI were Normalized (from −1 to 1) as they had different ranges and hence could not be compared. From the seasonal indices, the pigeon peas planting season (July to September) was singled out as the most important season to study agricultural droughts. The planting season analysis selected all years with severe conditions (2008, 2009, 2010, 2011, 2017 and 2022) for spatial analysis. Spatial analysis revealed that most areas in the upstream part of the Basin and Coastal region in the lowlands experienced severe to extreme agricultural droughts in highlighted drought years. The modelled agricultural drought results were validated using yield data from two stations in the Basin. The results show that the model performed well with a Pearson Coefficient of 0.87 and a Root Mean Square Error of 0.29. This proactive approach aims to ensure food security, especially in scenarios where the Basin anticipates significantly reduced precipitation affecting water available for agriculture, enabling policymakers, water resource managers and agricultural sector stakeholders to equitably allocate resources and mitigate the effects of droughts in the most affected areas to significantly reduce the socioeconomic drought that is amplified by agricultural drought in rainfed agriculture river basins.

1. Introduction

The Athi-Galana-Sabaki (AGS) basin plays a crucial role in agriculture. However, the Basin is significantly vulnerable to drought events due to its reliance on rainfed agriculture and diverse landscapes [1]-[3]. These droughts severely affect farmers who rely on rainfed agriculture to grow their crops, exposing them to reduced yields, income losses, and potential food insecurity [4] [5]. Also, reduced agricultural productivity due to drought negatively impacts the regional and national economy [6] [7]. In addition, droughts can exacerbate land degradation and affect water resources, leading to long-term environmental challenges [8]-[10].

Accurately quantifying and understanding the spatio-temporal dynamics of agricultural drought within the AGS basin is essential for addressing agricultural drought-induced challenges [11]. Traditional methods often lack the necessary detail or spatial coverage to effectively inform decision-making [12]. Hence, the main objective of this study is to quantify agricultural drought based on remote sensing data products available for precipitation (P), Land Surface Temperature (LST) and Normalized Difference Vegetation Index (NDVI) to highlight hotspot areas vulnerable to agricultural drought. The study of geospatial techniques and drought-specific indices like the Standardized Agricultural Drought Index (SADI) will aid in mapping and analyzing the spatial distribution and temporal evolution of agricultural drought severity across the Basin [13]-[15]. Quantifying the relationship between drought and crop yields to assess impacts on different agricultural systems is essential for informed planning against the drought effects [16]-[20]. Determining areas within the Basin most susceptible to drought is crucial for effectively using limited resources to provide more protection to the most vulnerable regions [21]-[23].

GIS and Remote Sensing technologies have emerged as powerful tools in combating agricultural droughts, empowering proactive and informed decision-making for farmers, policymakers, and stakeholders [24]. They provide data-driven insights that support informed decisions for drought preparedness, resource allocation, and targeted interventions. GIS and Remote Sensing are indispensable in mitigating agricultural droughts [25] [26].

Remote sensing provides real-time data on various parameters like rainfall, soil moisture, vegetation health, and LST [27]. These datasets help identify drought onset and monitor its progression across vast areas. By integrating climatic data with remote sensing information, GIS generates robust drought indices like NDVI anomaly, Standardized Precipitation Index (SPI), and Vegetation Condi-

tion Index (VCI) [27]-[29]. These indices quantify drought severity and predict potential impacts on crops, enabling early warnings for targeted responses [24]. GIS analyzes factors like soil types, topography, and historical drought patterns to identify areas most vulnerable to drought. This spatial understanding enables targeted interventions and resource allocation towards the most critical regions [30]. By overlaying climatic data with soil characteristics and historical yield information, GIS helps identify areas suitable for drought-resistant crops, promoting adaptive agricultural practices. High-resolution satellite imagery and drone data provide detailed insights into field-specific variations in crop health and water stress [31]. This allows for precision irrigation practices, optimizing water usage and minimizing losses [31] [32]. GIS analysis of land cover, water bodies, and soil infiltration rates helps design efficient water management strategies at the watershed level, optimizing water storage and distribution [33]. GIS creates intuitive maps and dashboards that effectively communicate drought severity, vulnerability, and mitigation strategies to diverse stakeholders, including farmers, policymakers, and extension service providers [34]. Real-time information and tailored advisories can be delivered directly to farmers through mobile applications, empowering them to adapt their practices based on drought conditions [35] [36].

The Agricultural Drought Index (ADI) is a comprehensive drought index specifically designed to assess drought impacts on agricultural systems [37]. Unlike other indices focusing solely on meteorological or hydrological variables, the ADI integrates various components related to agricultural productivity, soil moisture, and crop health [38]. While there is no standard formula for the ADI, it typically incorporates meteorological variables, LST and vegetation health [39].

Precipitation and temperature data are often included in the calculation of the ADI to assess rainfall deficits and temperature anomalies, both of which directly impact agricultural activities and crop growth [37]. Indices such as the NDVI and VCI are used to evaluate vegetation health and stress levels. Reduced vegetation health due to water deficits or temperature extremes can indicate agricultural drought conditions [40].

Some versions of the ADI may include crop-specific parameters or thresholds to tailor the index to the particular crops grown in the region of interest [41]. Different crops have varying sensitivities to drought, so incorporating crop-specific information enhances the relevance of the index for agricultural drought monitoring [30]. The ADI is often calculated using a weighted combination of these components, with weights assigned based on their relative importance and relevance to agricultural drought impacts [42].

The exact formula for the ADI may vary depending on the specific objectives of the assessment, data availability, and regional characteristics [43]. The ADI provides valuable information for decision-makers, farmers, and stakeholders involved in agricultural management. It allows them to assess drought risks, im-

plement mitigation measures, and make informed decisions to safeguard crop production and food security [44]. Its comprehensive nature makes it a useful tool for monitoring and managing agricultural drought conditions in diverse agroecological regions [45].

2. Materials and Methods

Base datasets for the study involve Landsat data and Climate Hazards Group InfraRed Precipitation with Station data (CHIRPS), with the other data revolving around these two data types. Data acquisition, being a key part of any project, acts as a starting point of the study with the acquisition of Landsat 7 and Landsat 8 data, which was the ultimate fit due to the time series duration of the analysis. The methodology shown in Figure 1 for the Agricultural Drought Monitoring System utilizing the ADI which involves a systematic process outlined in various stages as follows:

1) The Normalized Difference Vegetation Index

$$NDVI = \frac{(NIR - RED)}{(NIR + RED)} \tag{1}$$

where:

NIR = Near-Infrared reflectance. Vegetation reflects more near-infrared light compared to visible red light.

RED = Red reflectance. Vegetation absorbs more red light compared to near-infrared light.

$NDVI$ represents the output value of the index, ranging from −1 to +1.

2) Land Surface Temperature

LST refers to the temperature of the Earth's surface, as measured by remote sensing instruments like satellites. LST is typically measured in degrees Kelvin (K) or Celsius (°C). Satellites carry sensors that can detect the thermal radiation emitted by the Earth's surface. Scientists can estimate the LST of different land cover types by analyzing this radiation.

3) The Vegetation Condition Index

$$VCI = \frac{(NDVI - NDV_{Imin})}{(NDV_{Imax} - NDV_{Imin})} * 100\% \tag{2}$$

where:

NDV_{Imin} = Minimum $NDVI$ value observed for a specific pixel over a chosen historical reference period. This value signifies the lowest vegetation greenness recorded for that pixel.

NDV_{Imax} = Maximum $NDVI$ value observed for a specific pixel over the chosen historical reference period. This value signifies the highest vegetation greenness recorded for that pixel.

4) Temperature Condition Index

$$TCI = \frac{(T_{max} - T_{min})}{(T - T_{min})} * 100\% \tag{3}$$

where:

TCI is the Temperature Condition Index.

T is the temperature for a specific period (e.g., monthly, seasonal).

T_{min} is the minimum temperature over the same period.

T_{max} is the maximum temperature over the same period.

4) The Vegetation Health Index

$$VHI = 0.5*(VCI + TCI) \tag{4}$$

5) Standardization of VHI to Standardized Drought Index (SDI)

$$SDI = \frac{VHI - VHI_{\mu}}{VHI_{\sigma}} \tag{5}$$

where:

SDI is the Standardized Agricultural Index.

VHI_{μ} is the VHI mean.
VHI_{σ} is the VHI standard deviation.

6) Normalization of Agricultural index

$$SADI = 2*\frac{SDI - SDI_{min}}{SDI_{max} - SDI_{min}} - 1 \tag{6}$$

where:

SADI is the Standardized Agricultural Drought Index after normalization.

SDI_{min} is the minimum SDI.

SDI_{max} is the maximum SDI.

7) Standardized Precipitation Index

SPI is the widely used drought index that quantifies precipitation anomalies relative to a specified period and distribution. Its comprehensive formulae can be obtained in.

SPI can be summarised as follows:

$$SPI = \frac{X_i - \bar{x}}{\sigma} \tag{7}$$

where:

X_i is the precipitation value for the current period (e.g., monthly precipitation).

$\bar{x}$ is the long-term mean precipitation over the same time scale.

σ is the standard deviation of precipitation over the same time scale.

In the initial data collection and preparation phase, Landsat 7 and 8 satellite imagery for the AGS Basin were gathered from the Landsat image collection. The images were processed to mask out clouds and cloud shadows using a custom cloud masking function to ensure data accuracy. The study area was defined using the geographical boundaries of the AGS Basin delineated from the SRTM DEM basin using basin outlet coordinates.

Following data preparation, the temporal selection phase involves user input for the start and end years of the analysis. Additionally, a specific season (1 - 4) was chosen, with each season corresponding to 3 months as defined by rainfall

seasons. For Kenya, the seasons are categorized into three months per season as follows: first season (hot and dry season)—December to February; second season (long rain season)—March to May; third season (cool and dry)—June to August and fourth season (short rain season)—September to November [46]. For this study, the seasons have been slightly altered, shifting forward by one month to give January to March, April to June, July to September and October to December for a first, second, third and fourth season. The main reason for the shift is to accommodate the July to September pigeon peas growing season in the Basin.

In the Image Collection stage, the Landsat 7/8 collection was filtered based on the specified start and end months for the Galana Basin. Subsequently, essential vegetation indices, such as NDVI shown in Equation (1) [47] and VHI, were calculated to evaluate the agricultural landscape. The LST calculation phase involved deriving LST using Landsat 8 thermal bands, with a crucial step being the application of cloud masking. Emissivity was then calculated and utilized to adjust the LST values.

Vegetation Condition Indices (VCI, TCI, VHI) were computed in the subsequent phase. VCI shown in Equation (2) [48] was determined by the ratio of the difference between NDVI and its minimum to the range between its maximum and minimum. On the other hand, TCI was computed as the ratio of the difference between maximum and current LST to the range between maximum and minimum LST, as shown in Equation (3) [49]. Combining VCI and TCI provided the VHI calculated in Equation (4) [50]. The drought Index (SDI calculated in Equation (5)) [51] calculation phase involves classifying VHI values and standardizing and normalizing values (SADI computed in Equation (6)) [52] into specific classes based on threshold values, enabling the generation of a drought index map. Numeric values were assigned to these classes to facilitate further analysis.

The standardization of the drought index was carried out to ensure consistent scaling across different seasons. Standardized values for the Drought Index were computed using mean and range (−1 to 1) normalization techniques. The SPI calculation for the comparison stage required user input for the start and end years and the chosen season. SPI was computed in Equation (7) [53] using CHIRPS imagery, and the layers are displayed on the map for visual analysis.

3. Results

3.1. Parameter Evaluation

3.1.1. Digital Elevation Model
The Digital Elevation Model (DEM) of the Athi-Galana-Sabaki River Basin in Kenya was derived from the 90-metre Shuttle Radar Topography Mission (SRTM) dataset. The DEM shows the geomorphology of the area. The geomorphology shows how the topography is changing within the Basin. Analyzing the topographic characteristics of this Basin is essential for understanding water resources, land use planning, and disaster preparedness. The high-resolution
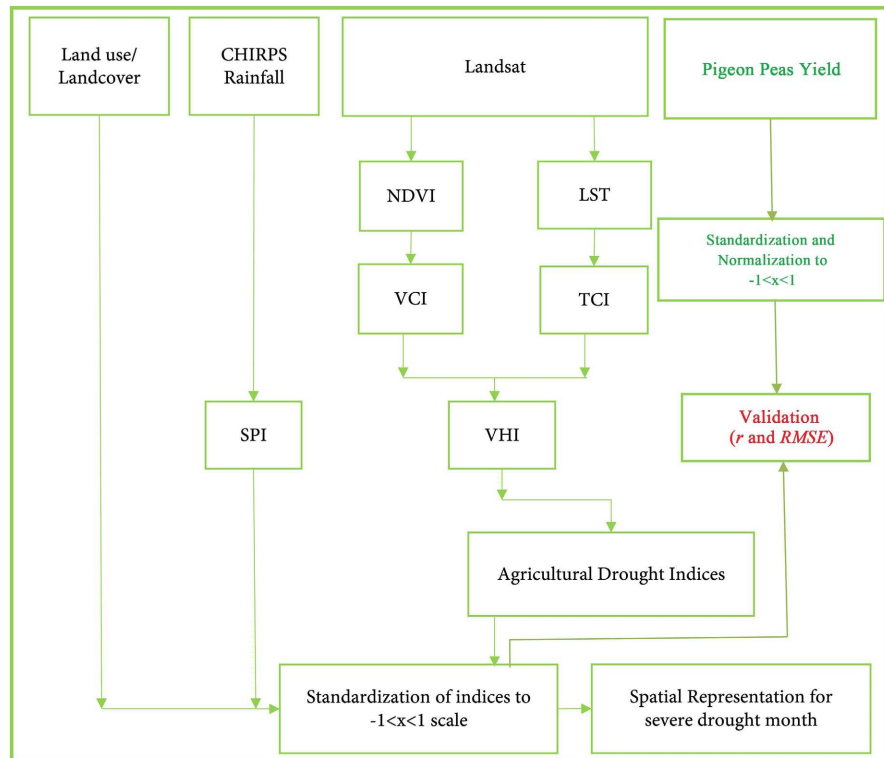
Figure 1. A flowchart showing how various sections of the methods are interlinked.

DEMs are available for the Athi-Galana-Sabaki basin, offering high levels of detail and accuracy. The DEM analysis of the Athi-Galana-Sabaki basin revealed valuable information about the topography, which involved analyzing slope gradients, identifying potential erosion-prone areas, and delineating areas suitable for various lands. The DEM also helped link droughts and the general undulation of the Basin. From the results, the DEM image of the area reveals that the AGS Basin has a varied topography, with high mountains or hills in the western and central regions, giving way to lower-lying plains and riverbeds in the eastern part. The basin elevation ranges from 0 metres above sea level (a.s.l) to 5801 metres a.s.l, as shown in **Figure 2**. The higher elevation values correspond to mountainous areas surrounding the Basin, while the lower values represent the basin floor at the coast. The AGS Basin's diverse elevation profile profoundly impacts its hydrology, environment, and land-use patterns. Understanding the Basin's elevation characteristics is crucial for effective water management, land-use planning, and disaster risk mitigation.

3.1.2. Rainfall

The AGS River Basin is a vital water source for Kenya's eastern region, supporting agriculture, industry, and urban populations. Rainfall is an essential resource for the ASG basin and a source of vulnerability. The Basin is characterized by uneven rainfall distribution, high seasonal variability, and sensitivity to climate variability. These factors challenge water management, disaster preparedness, and sustainable development. Effective management of water resources in the

ASG basin will require a comprehensive approach that addresses climate change, land degradation, and population growth. Understanding the Basin's rainfall patterns and variability is crucial for water resource management and sustainable development [54].

Rainfall in the ASG basin is distributed unevenly, with higher rainfall in the central highlands and lower rainfall in the southeast. Figure 3 shows that the average annual rainfall in the Basin is about 750 millimetres, which can vary considerably yearly. Rainfall distribution within seasons is also variable, with intense downpours interspersed with dry periods, leading to flash floods and soil erosion. Yearly rainfall amounts fluctuate considerably, with periodic droughts causing significant water stress. El Niño and La Niña events can influence rainfall patterns, with El Niño typically bringing increased rainfall and La Niña associated with droughts [55].

The mountainous regions receive the highest rainfall (2272 millimetres in Mt. Kilimanjaro region), and the areas are relatively flat. Those nested in the leeward side of the hilly regions receive low rainfall, as low as 356 millimetres, except for the areas near the coast that receive wet winds from the Ocean that promote rainfall, see Figure 4. The topography plays a significant role, with the eastern slopes of the Kenya Highlands receiving heavier rainfall due to the orographic lifting of moisture-laden winds [56].
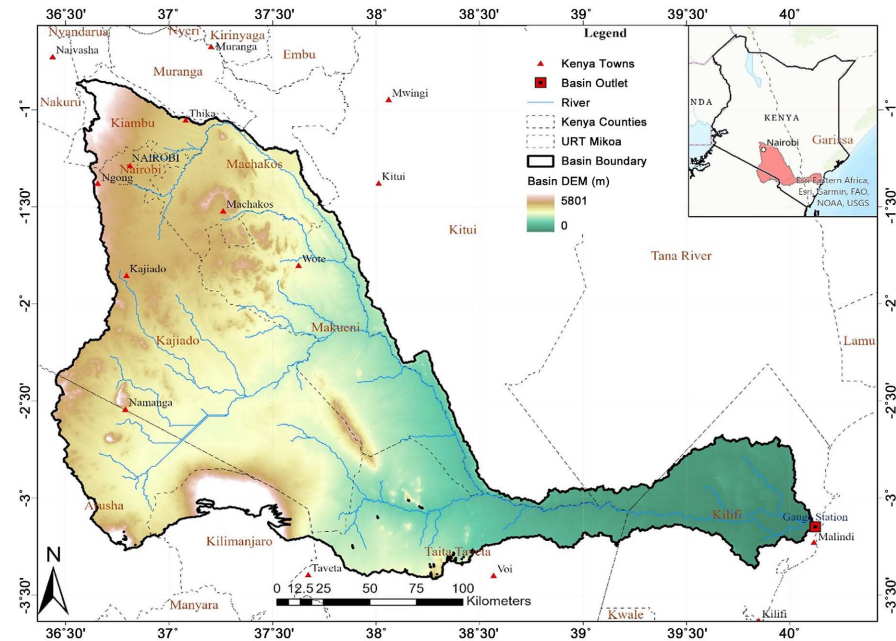

Figure 2. Map showing the Digital Elevation Model enhanced by Hill Shade.

3.1.3. Land Use Land Cover

The Athi-Galana-Sabaki River Basin, straddling Kenya's eastern highlands and coastal plains, represents a critical water resource for over 10 million people. Leveraging FAO data alongside other sources helps gain valuable insights into the LULC dynamics of the Athi-Galana-Sabaki river basin. This information is
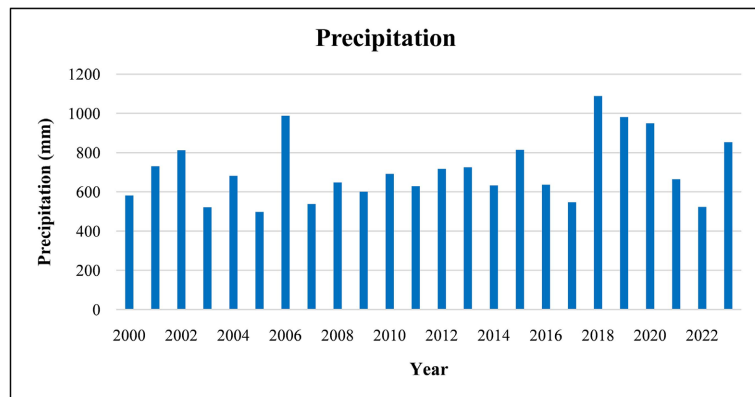
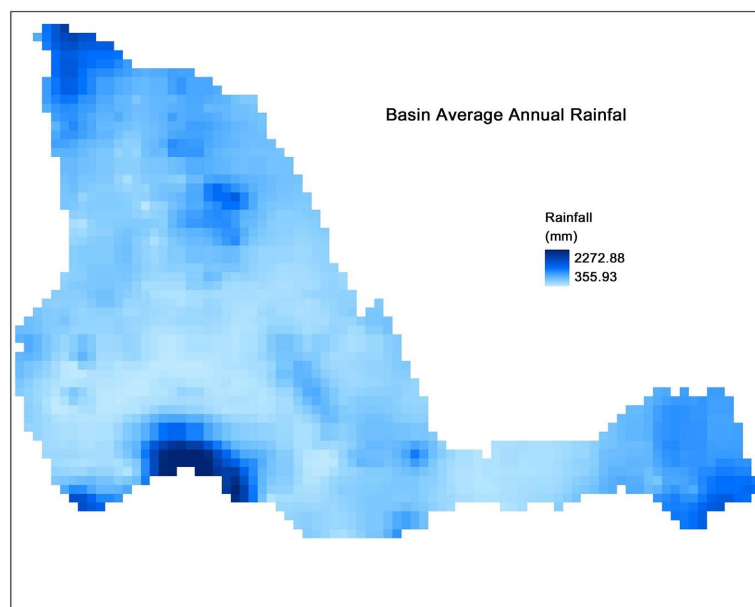**Figure 3.** Average annual rainfall temporal variability in AGS Basin.

Figure 4. Average annual rainfall spatial variability in AGS Basin.

essential for informed decision-making regarding water resource management, land degradation prevention, and promoting sustainable development in the region amid threats posed by climatic changes and hazards. Cognizant of the reasons mentioned above. This study analyses the LULC in the AGS Basin to support understanding and interpreting drought conditions in the Basin.

According to the FAO Global Land Cover (GLC) map in Figure 5, grasslands encompass about 65% of the Basin's area. These include savannas, shrublands, and grasslands used for pastoralism and wildlife conservation. Rainfed and irrigated agriculture constitutes roughly 20% of the Basin, concentrated in the upper and middle reaches. Tea and coffee plantations are prominent alongside maize, sorghum, and other subsistence crops. Dense forests, mainly montane forests in the upper catchment, cover around 5% of the Basin. Montane forests play a vital role in soil conservation and water regulation. Freshwater and estuarine wetlands occupy approximately 2% of the area, providing valuable ecologi-

cal services like flood mitigation and habitat for numerous bird species. Urban and rural settlements, including Nairobi city, account for roughly 3% of the Basin. The expansion of settlements raises concerns about water pollution and resource pressure. Open water bodies and bare land represent 5% of the Basin.

The LULC composition of the Athi-Galana-Sabaki River Basin, revealed by FAO data, highlights the complex interplay between human activities and environmental sustainability. Understanding these patterns and their implications is crucial for informing informed land-use planning, environmental conservation, and sustainable water management practices to ensure the Basin's future water security and ecological well-being.
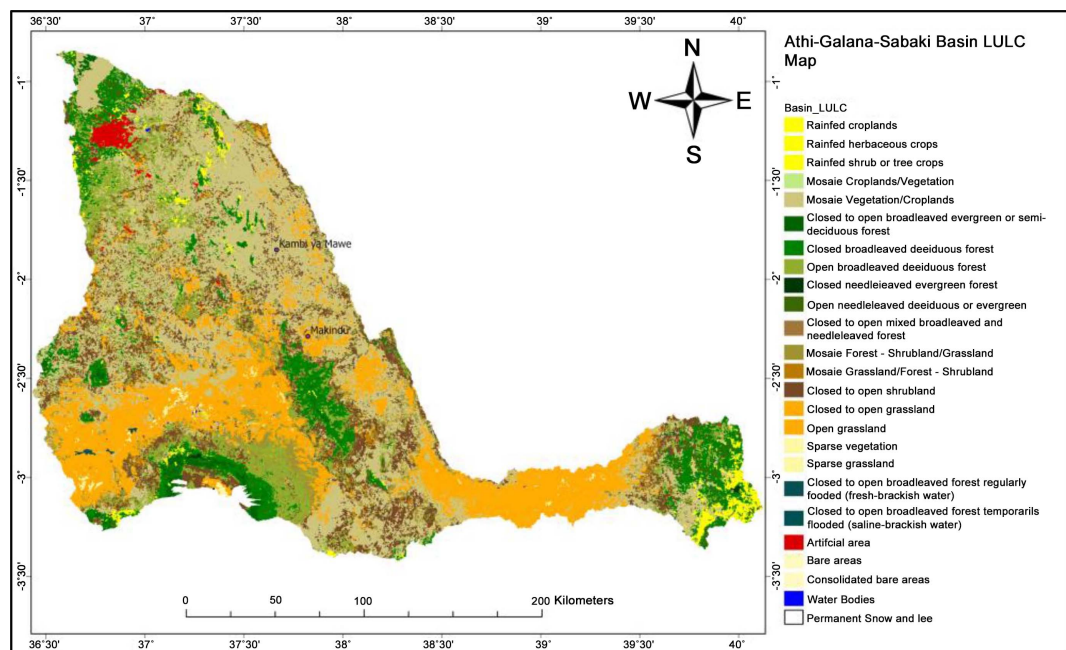

Figure 5. Athi-Galana-Sabaki Basin land use land cover spatial representation—the FAO extracted datasets and classes.

3.1.4. Impact of Evapotranspiration on Agricultural Drought

Evapotranspiration refers to the combined process of evaporation (water vaporization from soil and water surfaces) and transpiration (water loss through plant leaves). Evapotranspiration (ET) is a crucial process that connects soil, crops, and the atmosphere. It plays a significant role in the water cycle and energy exchange. Agricultural practices significantly impact ET. Crop types, irrigation methods, and soil management affect water availability and transpiration rates. For agriculture, understanding ET is essential for water management, especially in regions prone to drought [57].

From the results, Figure 6 shows that the average annual ET in the AGS basin is around 111.3 millimetres per year. However, there has been temporal variation in ET rates over the years. Similarly, Figure 7 shows that the spatial annual ET in the AGS basin ranges from 44.56 millimetres to 333.68 millimetres. However, there is spatial variation in ET rates across the Basin. Areas with higher ET

will likely have more dense vegetation or higher temperatures.

ET directly affects water availability in the soil. High ET rates in agricultural areas can lead to soil moisture depletion, especially during periods of limited precipitation, exacerbating drought conditions. Different land uses have varying vulnerabilities to drought. Agricultural lands, especially rainfed croplands, are particularly susceptible to drought due to their reliance on adequate soil moisture for crop growth. Understanding the relationship between ET and LULC is crucial for monitoring and mitigating agricultural drought. Remote sensing techniques, as illustrated in Figure 6 and Figure 7, can be used to monitor ET rates and changes in LULC, providing valuable information for drought early warning systems and water resource management strategies.

In summary, the relationship between evapotranspiration and land use/land cover is fundamental to understanding agricultural drought dynamics. Changes in land use can alter ET rates, affecting water availability and the vulnerability of agricultural systems to drought. Effective management strategies must consider these interactions to mitigate the impacts of agricultural drought.
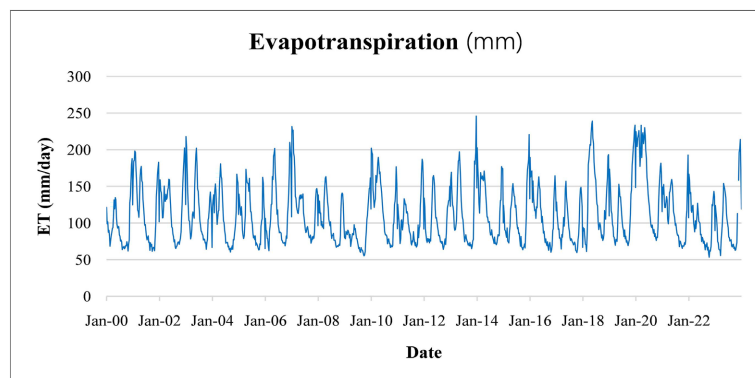

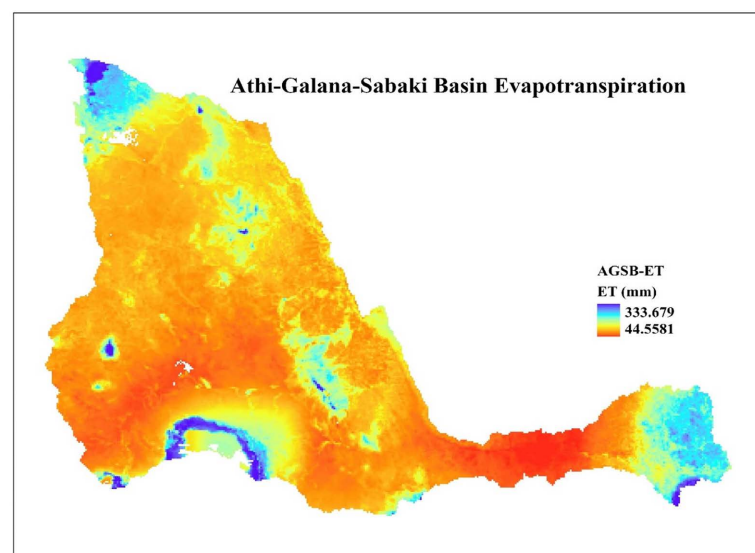**Figure 6.** Evapotranspiration temporal variability graph for AGS Basin.

Figure 7. Athi-Galana-Sabaki Basin evapotranspiration spatial representation.

3.1.5. Yield

Like other crops, Pigeon peas are susceptible to the impacts of agricultural drought, which can significantly affect their yield. Pigeon peas require adequate soil moisture for germination, vegetative growth, flowering, and pod development. During agricultural drought, soil moisture levels can decline, leading to soil moisture stress for pigeon pea plants. This stress can impair root development, nutrient uptake, and overall plant growth, reducing crop yield. Agricultural drought can disrupt pigeon pea plants' flowering and pod formation stages [58]. Insufficient soil moisture and water stress can lead to reduced flower production, poor pollination, and abortion of developing pods. As a result, the number of pods per plant and yield can be significantly reduced [59]. Drought stress can also impact the uptake of essential nutrients by pigeon pea plants. Reduced water availability in the soil limits the movement of nutrients to plant roots, leading to nutrient deficiencies that can further exacerbate yield losses. Severe drought stress can trigger premature senescence in pigeon pea plants, where leaves can turn yellow and drop prematurely, reducing the plant's photosynthetic capacity. This premature ageing can limit the plant's ability to fill pods and develop seeds, resulting in lower crop yield at harvest. Drought-stressed plants are often more vulnerable to pest infestations and diseases. Pigeon pea crops experiencing drought stress may be more susceptible to pest attacks such as pod borers and diseases like Fusarium wilt, further compromising yield potential [60]. Chronic agricultural drought can have long-term consequences for soil health, including soil erosion, depletion of organic matter, and degradation of soil structure. These soil degradation processes can negatively affect the productivity of pigeon pea crops in subsequent growing seasons [58].

The data that was available for a long period having pigeon peas yield data was for two stations, Kambi ya Mawe and Makindu. It is important to note that, for such a study, the yield data must be comparable, and thus, it requires data from at least two stations in the same ecological zone. Makindu and Kambi ya Mawe stations were favored in this study because they are in the same ecological zone. The two locations have research stations that monitor yield under various conditions. The data used in Figure 8 and Figure 9 is the water-limited yield potential data referring to the rainfed agricultural yield that is crucial in understanding the relationship between drought and crop yield. The two stations in the same ecological zone show different results pointing to spatial variability of pigeon peas growth enabling factors and, more so, soil moisture availability exacerbated by climate change. For Makindu station, the lowest yield was recorded in 2009 (0.8 t/ha/year), and the highest yield was recorded in 2002 (4.0 t/ha/year) with an average of 2.5 t/ha/year. Kambi ya Mawe station's lowest yield was recorded in the year 2012 (1.2 t/ha/year), and the highest yield was recorded in 2010 (5.0 t/ha/year) with an average of 3.1 t/ha/year, showing a better yield compared to Makindu data. The data from the two stations show interannual variation, which can help with interpretation by location-based SADI.
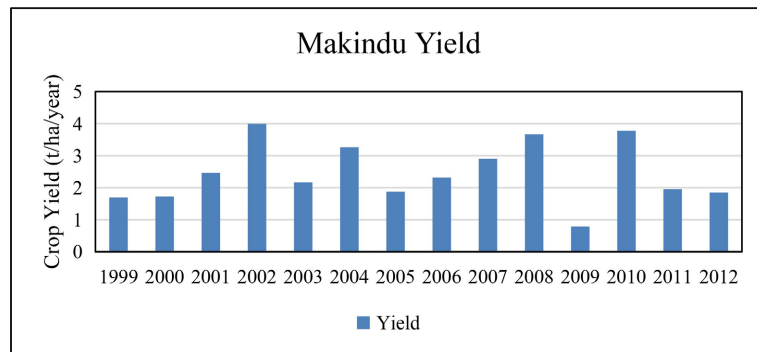
Figure 8. Makindu pigeon peas yield in tonnes per hectare per year from 1999 to 2012.
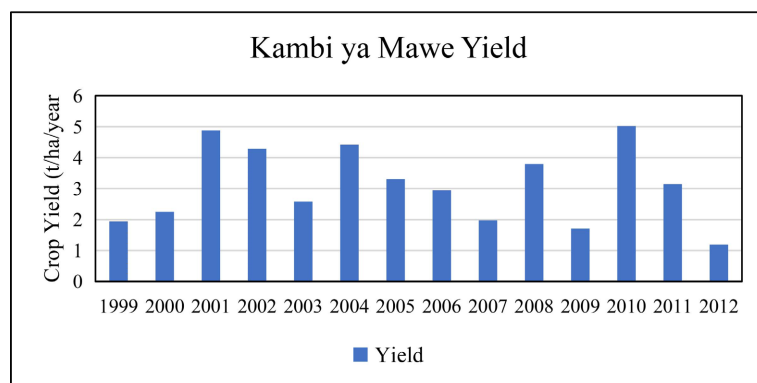

Figure 9. Kambi ya Mawe pigeon peas yield in tonnes per hectare per year from 1999 to 2012.

3.2. Modelling Drought Indices

The results obtained from the analysis offer valuable insights into SPI and SADI over the period from 2000 to 2023. These indices are fundamental to the study's methodology, aligning with the overarching goal of drought risk assessment and mitigation planning in the AGS River Basin. The SPI measures meteorological drought, capturing deviations in precipitation from historical norms, while the SADI focuses on agricultural drought, considering variables such as vegetation health and land surface temperature [61]. It is important to note that in a perfect scenario, the normalized SPI and SADI should be equal in the ideal case. That was not the case in this study, as SADI has other external factors altered its results.

The seasonal breakdown of the results, covering four seasons each year, allows for a comprehensive evaluation of drought conditions throughout the years under consideration. Examining the temporal variations in SPI and SADI values revealed dynamic patterns, highlighting fluctuations in meteorological and agricultural drought conditions. Negative SPI values indicate periods of below-average precipitation, indicative of meteorological drought, while negative SADI values underscore agricultural drought conditions and their impact on vegetation and surface conditions. Conversely, positive values suggest relatively

normal or above-average conditions in both indices.

The comparison of SPI and SADI values for the same seasons provides insights into spatial correlations or disparities between meteorological and agricultural drought. Consistent patterns or deviations between the two indices offer valuable information for understanding the interplay between meteorological factors and their downstream impact on agriculture.

As illustrated in the methodology, the seasonal SADI was computed by combining various biophysical properties. The seasonal SADI values were plotted in a bar chart, as shown in Figure 10, with more focus on season three (planting season). Several key seasons from the results stand out, providing noteworthy insights into meteorological and agricultural drought dynamics in the Galana River Basin. For instance, in 2002, Season 4 exhibited a remarkable positive shift in SPI and SADI values. This suggests a period of above-average precipitation and improved agricultural conditions, emphasizing the interconnection between meteorological factors and positive outcomes for agriculture.

Analyzing season three in Figure 10, it was noted that only six years had extreme or severe droughts. The years highlighted were 2008, 2009, 2010, 2011, 2017 and 2022. The drought years identified were further prepared for spatial analysis to give more insights into the spatial variability of the drought within the Basin.

In this analysis, the three-month moving average was favoured mainly because of its capability to capture short to medium-term variations in precipitation, which are often relevant for assessing agriculture. It provides a balance between capturing recent precipitation anomalies and smoothing out short-term fluctuations. In addition, a three-month average aligns well with critical stages of the crop growth cycle, including germination, vegetative growth, and reproductive stages. By considering precipitation over this timeframe, SPI can provide insights into how current conditions may impact crop yields and water availability for irrigation.

The normalized values of SADI and SPI were plotted together to visually compare the two indices, as shown in Figure 11. From the result, it can be observed that SADI and the normalized SPI values do not align perfectly, as pointed out earlier, mainly because of other external factors that cause variations in SADI. Even though they do not have the same values, it can be noted that the two indices agree on the general trend of the drought. The two indices indicated severe droughts in 2009, 2010, 2011 and 2022 but different results for 2014, 2016, 2017 and 2019. The slight differences point to the cautious use of SPI in agricultural monitoring, as crop water demand is not the only factor influencing vegetation growth and phenology.

3.3. Agricultural Drought Hotspot Mapping

Spatial analysis of agricultural drought plays a crucial role in understanding, monitoring, and responding to drought impacts on agriculture and rural communities. By leveraging spatial data and analytical tools, stakeholders can
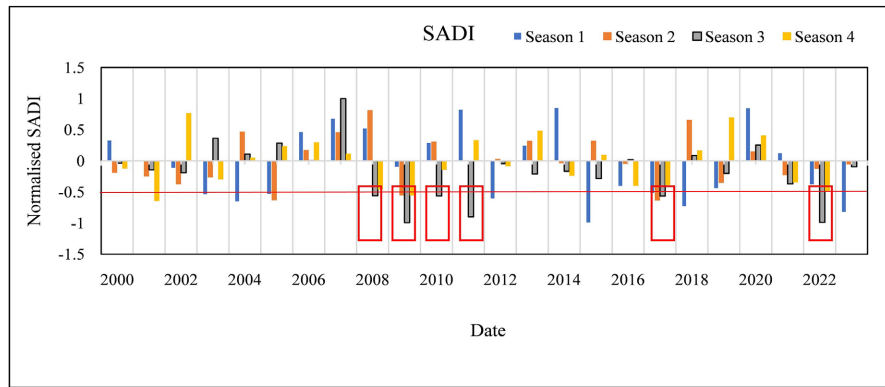
Figure 10. SADI for AGS River Basin is computed per season. Season three, during which pigeon peas grow, was the main focus, with years of season three SADI below −0.5 highlighted for spatial analysis.
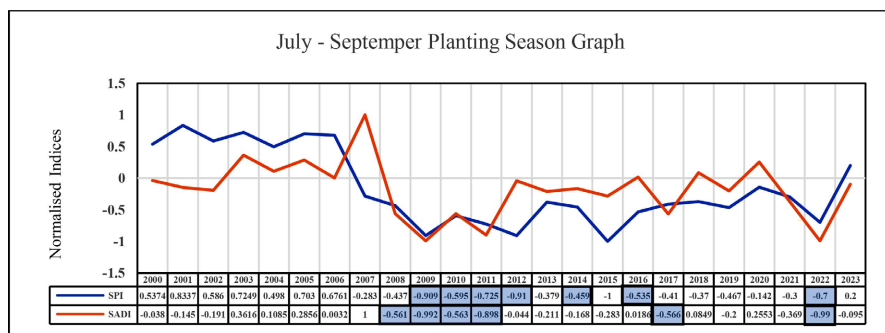

	2000	2001	2002	2003	2004	2005	2006	2007	2008	2009	2010	2011	2012	2013	2014	2015	2016	2017	2018	2019	2020	2021	2022	2023
SPI	0.5374	0.8337	0.586	0.7249	0.498	0.703	0.6761	-0.283	-0.437	-0.909	-0.595	-0.725	-0.91	-0.379	-0.459	-1	-0.535	-0.41	-0.37	-0.467	-0.142	-0.3	-0.7	0.2
SADI	-0.038	-0.145	-0.191	0.3616	0.1085	0.2856	0.0032	1	-0.561	-0.992	-0.563	-0.898	-0.044	-0.211	-0.168	-0.283	0.0186	-0.566	0.0849	-0.2	0.2553	-0.369	-0.99	-0.095

Figure 11. Comparison of SADI and SPI indices for AGS River Basin season three data from 2000 to 2023.

enhance their capacity to assess, mitigate, and adapt to the complex spatial dynamics of agricultural drought. Hence, this study investigates areas prone to droughts to support intervention efforts to mitigate the effect of droughts and prepare for future droughts.

To understand droughts in the AGS River Basin, the spatial distribution of drought in the Basin was mapped per pixel, 5 kilometres by 5 kilometres unit areas for SADI drought years (2008, 2009, 2010, 2011, 2017 and 2022). **Figure 12(a)** and **Figure 12(b)** give the spatial distribution of the 2008 and 2009 drought, respectively; the spatial distribution shows severe drought conditions in most parts of the Basin. The area received almost the same drought conditions throughout the Basin as the area responded to the shocks of reduced precipitation. In the third season of 2009, the areas that received high rainfall were the most affected by extreme drought. These areas included mountainous regions, highland, hilly and coastal areas primarily found in the western, southern, and coastal regions. Notably, the generally dry areas, mostly inhabited by grassland, only experienced mild drought. These results show that drought severely affected most farmers because most agricultural deficiencies were felt in arable land areas, as shown in **Figure 12(b)**. According to other studies, the 2008-2009 drought was caused by a combination of factors, including below-average rainfall, poor agricultural

practices, land degradation, and conflict-induced displacement of populations in some regions [62]. The drought exacerbated food insecurity and water scarcity in many parts of Kenya, particularly in arid and semi-arid areas [1] [62] [63].

The 2009 findings portrayed a scenario where the eastern part of the Basin faced a significant impact of severe and moderate agricultural drought during the short rains season. Taita Taveta County, in the southern part, encountered moderate drought, while the western regions, comprising Makueni, Mbooni, and Kibwezi, experienced low agricultural drought. This spatial distribution underscores the varied nature of drought across different regions within the Basin during the specified year.

2010, the situation was similar to other years; only in 2010 did coastal regions and areas around Mt. Kilimanjaro experience agricultural droughts, as shown in Figure 12(c). Figure 12(d) shows that 2011 findings portrayed a scenario where the eastern part of the Basin faced a significant impact of severe and moderate agricultural drought during the short rains season. Taita Taveta County, in the southern part, encountered moderate drought, while the western regions experienced extreme agricultural drought in highland areas that could have posed a serious challenge to farmers. This spatial distribution underscores the varied nature of drought across different regions within the Basin during the specified year. Extreme drought for 2017 concentrated mostly in the Western part of the Basin, with moderate drought conditions being felt throughout the Basin, as shown in Figure 12(e), mainly due to low precipitation experienced and high LST recorded during this period. Like 2009, 2022 experienced extreme drought, which affected most arable land areas, although the 2009 drought had more intensity. The 2022 drought mainly affected the central and coastal regions of the Basin, as shown in Figure 12(f).

The hilly and mountainous areas and the coastal regions have been constantly affected throughout the analyzed drought years mainly because mountains and hills can create rain shadows, where prevailing winds pick up moisture from one side of the mountain but release it as precipitation on the windward side, leaving the leeward side relatively dry. This phenomenon can result in reduced rainfall and increased aridity on the leeward slopes and valleys, making these areas more susceptible to droughts. Coastal regions often experience lower and more erratic rainfall compared to inland areas. This is partly due to the influence of nearby oceans, which can inhibit precipitation formation or lead to coastal fog and low cloud cover that restricts rainfall. As a result, coastal areas may be more prone to experiencing drought conditions, especially during reduced or failed rainy seasons [64].

Furthermore, hilly areas and mountainous regions often exhibit diverse terrain and microclimates due to elevation, aspect, and slope variations. These variations can lead to spatial heterogeneity in precipitation patterns, with some areas receiving higher rainfall while others experience lower precipitation amounts. Consequently, areas with lower precipitation are more prone to droughts, espe-

cially during periods of reduced rainfall [13].
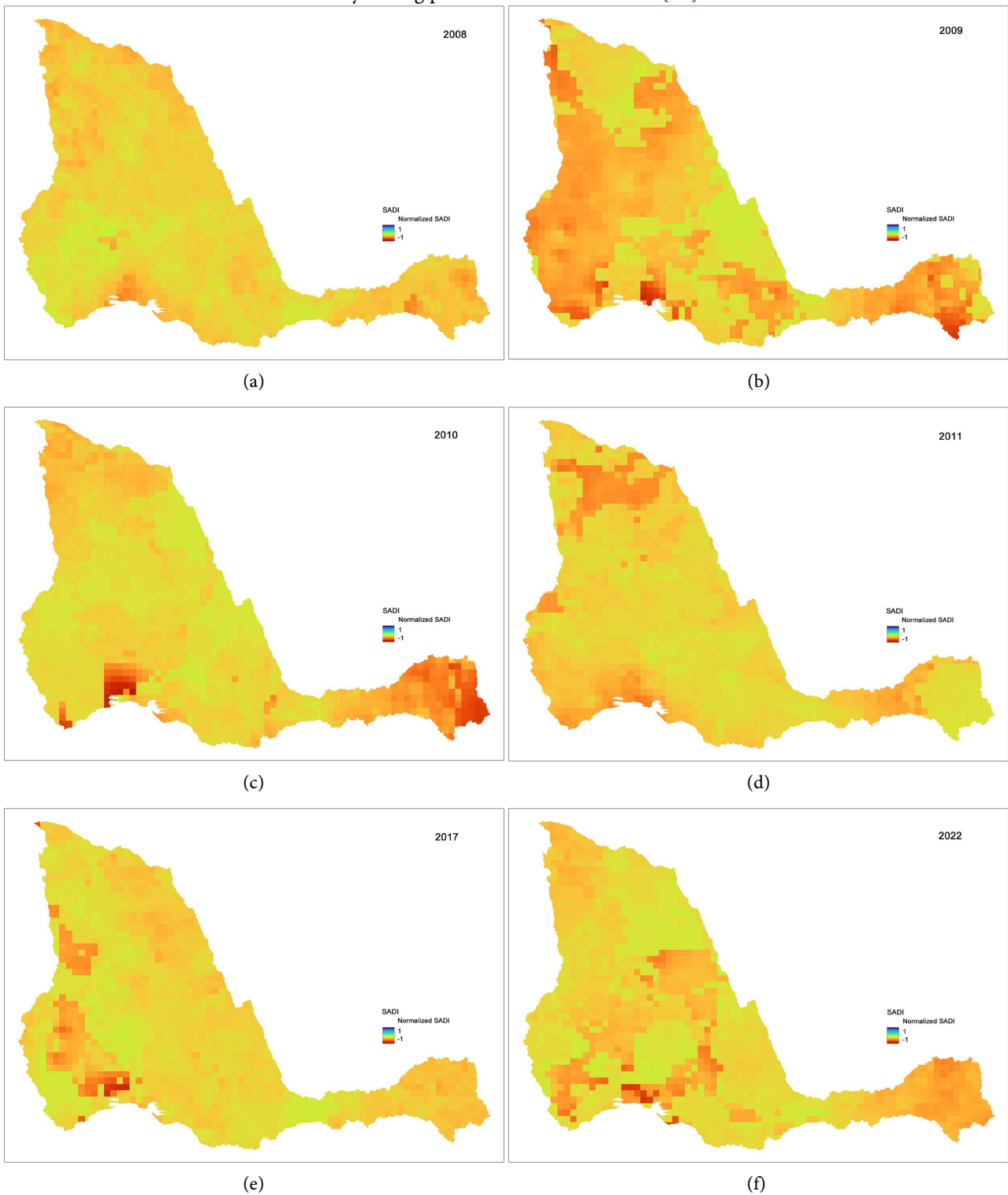

Figure 12. AGS River Basin Standardized Agricultural Drought Index spatial variability for various droughts as follows: (a) SADI for 2008, (b) SADI for 2009, (c) SADI for 2010, (d) SADI for 2011, (e) SADI for 2017 and (f) SADI for 2022.

The results from the analysis serve as a foundation for informed decision-making in drought mitigation. Identifying periods of heightened risk, such

as consecutive seasons with negative SPI and SADI values, prompts the need for targeted interventions in agriculture, water management, and community planning, especially in the Basin's highlands, coastal, and mountainous and hilly areas. In conclusion, when interpreted alongside the project's methodology and background, the analysis outcomes contribute to a nuanced understanding of drought dynamics in the Galana River Basin, facilitating comprehensive risk mitigation and resource allocation strategies.

3.4. Validation of Agricultural Drought Using Observed Yield

The agricultural drought conditions and yield analysis revealed valuable insights into the relationship between weather patterns, crop performance, and agricultural productivity. The yield data from the two stations (Kambi ya Mawe and Makindu) were also standardized and normalized to a range of $-1 < x < 1$ to allow comparison with the normalized SADI. From the results of the comparison, as shown in Figure 13 and Figure 14, there is a close relationship between agricultural drought conditions extracted from satellite data-based biophysical properties and the yield, and this relationship can be used to validate modelled agricultural drought indices using yield data. Other parameters like soil properties, crop genetics and varieties, crop management practices, water management, nutrient management, and pest and disease management are important in agricultural production, resulting in the observed differences between SADI and Yield Index. The results show that Kambi ya Mawe and Makindu have different production even though they are in the same ecological zone.

From statistical analysis, the validation results gave a Pearson Correlation (r) of 0.87 and a Root Mean Square Error (RMSE) of 0.29. r indicates a strong positive linear relationship between the SADI and yield index. In simpler terms, the yield index also tends to increase as SADI increases, and vice versa. A value of 1 would indicate a perfect positive linear relationship, and −1 would indicate a perfect negative linear relationship. Generally, a correlation coefficient closer to 1 (or −1) indicates a stronger linear relationship. RMSE indicates a better fit between the model and the data. The RMSE measures the average magnitude of the difference between predicted and actual values [65]. In this case, an RMSE of 0.29 suggests that the model's predictions are typically within 0.29 units of the actual values.

By comparing drought conditions, such as precipitation deficits or soil moisture anomalies, to crop yield data, it becomes possible to assess the direct impact of drought on agricultural productivity. This analysis can quantify the extent to which yield losses are attributable to drought events and provide insights into the severity and spatial distribution of drought impacts on different crops and regions [66].

Analyzing the temporal relationship between drought occurrence and crop yield fluctuations over multiple growing seasons or years can identify recurring patterns and trends [67]. For example, it may reveal whether certain types of

droughts (e.g., early-season droughts vs. mid-season droughts) have a more significant impact on yield and whether the frequency or intensity of droughts is increasing over time.

Examining the spatial distribution of drought conditions and crop yields across different geographical regions allows for the identification of areas particularly vulnerable or resilient to drought. It can highlight hotspots of drought impact where targeted interventions may be needed to support affected farmers and mitigate yield losses [19].
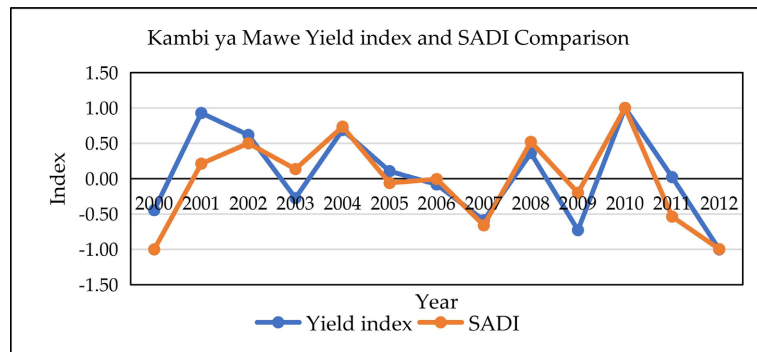

Figure 13. Kambi ya Mawe SADI and standardized pigeon peas yield index comparison from 2000 to 2012.
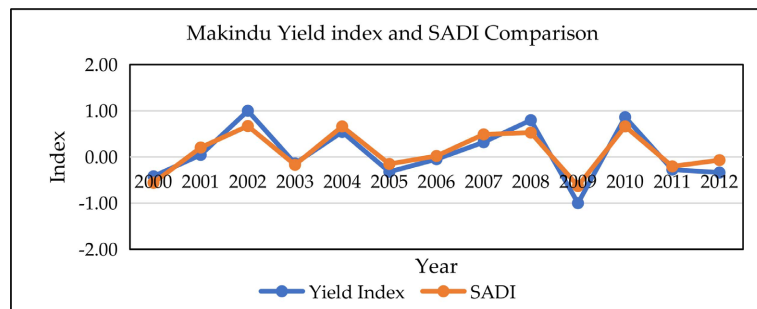

Figure 14. Makindu SADI and standardized pigeon peas yield index comparison from 2000 to 2012.

4. Discussion

The study systematically analyzed agricultural drought in the AGS River Basin, employing a robust methodology incorporating GIS and indices like SPI and SADI. The comprehensive approach to data collection, temporal analysis, and spatial visualizations has provided a nuanced understanding of drought dynamics in the region. The results presented provide a comprehensive understanding of agricultural drought in the Basin from 2000 to 2023, utilizing the SPI and SADI. The drought years identified were selected for detailed spatial visualizations, revealing varying intensities across different regions and emphasizing the spatial heterogeneity of agricultural drought impacts. The integration of GIS technology enhances the analysis by considering geographic features and environmental data attributes.

The identified key seasons in 2008, 2009, 2010, 2011, 2017, and 2022 for further visualizations align with the project's objective of determining drought-affected areas. The map visuals for these years reveal varying intensities of drought across different regions, emphasizing the spatial heterogeneity of agricultural drought impacts in the Basin. The findings underscore the importance of a nuanced understanding of drought dynamics for effective mitigation and planning strategies.

The SADI system proved to be a valuable tool for monitoring agricultural drought in the AGS River Basin, specifically for pigeon pea crops that were used to validate the drought index, which gave consistent results with r giving a value of 0.87 and $RMSE$ of 0.29. SADI provides a more objective and data-driven approach to drought monitoring than traditional methods relying on rainfall data alone. SADI effectively utilized satellite-derived data, likely vegetation indices (VIs) sensitive to plant health and moisture stress, to assess drought conditions in the Basin. By analyzing SADI outputs, agricultural stakeholders in the AGS basin can gain insights into the spatial extent and severity of drought stress impacting pigeon pea crops, timely identification of drought-affected areas, allowing for targeted interventions and improved decision-making regarding irrigation practices, resource allocation, and potential crop insurance claims.

5. Conclusions

The findings from this study have practical implications for hazard mitigation planning, risk assessment, and early detection systems. The study's integration of historical occurrences, frequency analysis, and vulnerability assessments aligns with its objective of offering a holistic approach to reducing drought risk. By highlighting drought hotspot areas, the study can be used to address the adverse effects on pasturelands, surface water basins, and crop production. The study provides actionable insights for public and private agencies to implement pre- and post-drought mitigation measures, highlighting the importance of education and outreach programs for mapped-out hotspot areas to enhance community resilience. Understanding the geomorphological and climatological conditions is crucial for sustainable water management, land use planning, and environmental conservation in the AGS River Basin.

In the broader context, the documentation and visualizations contribute to the understanding of agricultural drought monitoring and risk reduction, offering stakeholders and policymakers valuable information to formulate effective strategies for mitigating the impact of drought in the Basin. Overall, the project underscores the importance of a proactive and informed approach to address the complex challenges posed by agricultural drought in the region.

While SADI offers valuable insights, ground-based data collection (e.g., soil moisture measurements) can further validate SADI outputs and improve drought assessments. Tailoring SADI's algorithms to the specific spectral response of pigeon peas or any other crop can potentially enhance the accuracy of drought

detection for this crop. The utilization of the Standardized Precipitation Index (SPI) and the Standardized Anomaly Drought Index (SADI) for drought quantification presents methodological limitations and uncertainties. These include dependencies on the sensitivity to spatial and temporal scales, assumptions of stationarity amidst shifting climate patterns, subjective threshold selection, limited representation of hydrological processes, propagation of uncertainties throughout calculations, and oversimplification of the complex nature of drought phenomena [68]. Despite their usefulness, these indices necessitate cautious interpretation and integration with complementary monitoring methods to mitigate their limitations effectively and provide accurate drought assessments [69]. Combining SADI data with weather forecasts, climate models, and historical drought patterns can provide a more comprehensive picture of drought risks in the AGS River Basin.

Conflicts of Interest

The authors declare no conflicts of interest regarding the publication of this paper.

References

[1] Adam, B., Notkin, B., Konjhodzic, I., Undeland, E.I., Petrescu, D., Martin, M.A.D.C., Dione, O., Zerihun, A., Yicheneku, G.W. and Vermehren, A. (2022) Understanding Compound Events in Fragile Contexts Insights from Ethiopia & Kenya©. 2022 International Bank for Reconstruction and Development/The World Bank.

[2] Cai, X., Molden, D., Mainuddin, M., Sharma, B. and Karimi, P. (2013) Producing More Food with Less Water in a Changing World: Assessment of Water Productivity in 10 Major River Basins. *Water International*, **36**, 42-62.

[3] Zagade, N.D. and Umrikar, B.N. (2020) Drought Severity Modeling of Upper Bhima River Basin, Western India, Using GIS-AHP Tools for Effective Mitigation and Resource Management. *Natural Hazards*, **105**, 1165-1188.
https://doi.org/10.1007/s11069-020-04350-9

[4] Ahmad, M.M., Yaseen, M. and Saqib, S.E. (2022) Climate Change Impacts of Drought on the Livelihood of Dryland Smallholders: Implications of Adaptation Challenges. *International Journal of Disaster Risk Reduction*, **80**, Article ID: 103210.
https://doi.org/10.1016/j.ijdrr.2022.103210

[5] Mbuli, C.S., Fonjong, L.N. and Fletcher, A.J. (2021) Climate Change and Small Farmers' Vulnerability to Food Insecurity in Cameroon. *Sustainability*, **13**, Article 1523. https://doi.org/10.3390/su13031523

[6] García-León, D., Standardi, G. and Staccione, A. (2021) An Integrated Approach for the Estimation of Agricultural Drought Costs. Land Use Policy, **100**, 104923.
https://doi.org/10.1016/j.landusepol.2020.104923

[7] Naumann, G., Cammalleri, C., Mentaschi, L. and Feyen, L. (2021) Increased Economic Drought Impacts in Europe with Anthropogenic Warming. *Nature Climate Change*, **11**, 485-491. https://doi.org/10.1038/s41558-021-01044-3

[8] Hermans, K. and McLeman, R. (2021) Climate Change, Drought, Land Degradation and Migration: Exploring the Linkages. *Current Opinion in Environmental Sustai-*

nability, **50**, 236-244. https://doi.org/10.1016/j.cosust.2021.04.013

[9]   Orimoloye, I.R., Belle, J.A., Orimoloye, Y.M., Olusola, A.O. and Ololade, O.O. (2022) Drought: A Common Environmental Disaster. *Atmosphere*, **13**, Article 111. https://doi.org/10.3390/atmos13010111

[10]   Roy, P., Pal, S.C., Chakrabortty, R., Saha, A. and Chowdhuri, I. (2022) RETRACTED: A Systematic Review on Climate Change and Geo-Environmental Factors Induced Land Degradation: Processes, Policy-Practice Gap and Its Management Strategies. *Geological Journal*, **58**, 3487-3514. https://doi.org/10.1002/gj.4649

[11]   Ali, U., Shamsi, M.H., Bohacek, M., Purcell, K., Hoare, C., Mangina, E., *et al.* (2020) A Data-Driven Approach for Multi-Scale GIS-Based Building Energy Modeling for Analysis, Planning and Support Decision Making. *Applied Energy*, **279**, Article ID: 115834. https://doi.org/10.1016/j.apenergy.2020.115834

[12]   Sharma, N.N., Tapas, M.R. and Kumar, A.U. (2022) Drought Monitoring Indices. *Meteorology and Climatology*, **53**, 53-70.

[13]   Bhaga, T. (2021) Multispectral Remote Sensing of the Impacts of Drought and Climate Variability on Water Resources in Semi-Arid Regions of the Western Cape, South Africa. Master Thesis, University of the Western Cape, South Africa. https://etd.uwc.ac.za/bitstream/handle/11394/8612/bhanga_m_nsc_2021.pdf?sequence=1&isAllowed=y

[14]   Bhaga, T.D., Dube, T., Shekede, M.D. and Shoko, C. (2020) Impacts of Climate Variability and Drought on Surface Water Resources in Sub-Saharan Africa Using Remote Sensing: A Review. *Remote Sensing*, **12**, Article 4184. https://doi.org/10.3390/rs12244184

[15]   Chivangulula, F.M., Amraoui, M. and Pereira, M.G. (2023) The Drought Regime in Southern Africa: A Systematic Review. *Climate*, **11**, Article 147. https://doi.org/10.3390/cli11070147

[16]   Clarke, D., Hess, T.M., Haro-Monteagudo, D., Semenov, M.A. and Knox, J.W. (2021) Assessing Future Drought Risks and Wheat Yield Losses in England. *Agricultural and Forest Meteorology*, **297**, Article ID: 108248. https://doi.org/10.1016/j.agrformet.2020.108248

[17]   Cruz, M.G., Hernandez, E.A. and Uddameri, V. (2021) Vulnerability Assessment of Agricultural Production Systems to Drought Stresses Using Robustness Measures. *Scientific Reports*, **11**, Article No. 21648. https://doi.org/10.1038/s41598-021-98829-5

[18]   Frischen, J., Meza, I., Rupp, D., Wietler, K. and Hagenlocher, M. (2020) Drought Risk to Agricultural Systems in Zimbabwe: A Spatial Analysis of Hazard, Exposure, and Vulnerability. *Sustainability*, **12**, Article 752. https://doi.org/10.3390/su12030752

[19]   Meza, I., Eyshi Rezaei, E., Siebert, S., Ghazaryan, G., Nouri, H., Dubovyk, O., *et al.* (2021) Drought Risk for Agricultural Systems in South Africa: Drivers, Spatial Patterns, and Implications for Drought Risk Management. *Science of the Total Environment*, **799**, Article ID: 149505. https://doi.org/10.1016/j.scitotenv.2021.149505

[20]   Williams, T.G., Guikema, S.D., Brown, D.G. and Agrawal, A. (2020) Resilience and Equity: Quantifying the Distributional Effects of Resilience-Enhancing Strategies in a Smallholder Agricultural System. *Agricultural Systems*, **182**, Article ID: 102832. https://doi.org/10.1016/j.agsy.2020.102832

[21]   Alharbi, R.S., Nath, S., Faizan, O.M., Hasan, M.S.U., Alam, S., Khan, M.A., *et al.* (2022) Assessment of Drought Vulnerability through an Integrated Approach Using AHP and Geoinformatics in the Kangsabati River Basin. *Journal of King Saud Uni-*

versity—Science, **34**, Article ID: 102332. https://doi.org/10.1016/j.jksus.2022.102332

[22] Kimwatu, D.M., Mundia, C.N. and Makokha, G.O. (2021) Developing a New Socio-Economic Drought Index for Monitoring Drought Proliferation: A Case Study of Upper Ewaso Ngiro River Basin in Kenya. *Environmental Monitoring and Assessment*, **193**, Article No. 213. https://doi.org/10.1007/s10661-021-08989-0

[23] King-Okumu, C., Tsegai, D., Pandey, R.P. and Rees, G. (2020) Less to Lose? Drought Impact and Vulnerability Assessment in Disadvantaged Regions. *Water*, **12**, Article 1136. https://doi.org/10.3390/w12041136

[24] van Ginkel, M. and Biradar, C. (2021) Drought Early Warning in Agri-Food Systems. *Climate*, **9**, Article 134. https://doi.org/10.3390/cli9090134

[25] Hu, L., Zhang, C., Zhang, M., Shi, Y., Lu, J. and Fang, Z. (2023) Enhancing FAIR Data Services in Agricultural Disaster: A Review. *Remote Sensing*, **15**, Article 2024. https://doi.org/10.3390/rs15082024

[26] Surendran, U., Nagakumar, K.C.V. and Samuel, M.P. (2024) Remote Sensing in Precision Agriculture. In: Priyadarshan, P.M., Jain, S.M., Penna, S. and Al-Khayri, J.M., Eds., *Digital Agriculture: A Solution for Sustainable Food and Nutritional Security*, Springer, 201-223. https://doi.org/10.1007/978-3-031-43548-5_7

[27] Bento, V.A., Gouveia, C.M., DaCamara, C.C., Libonati, R. and Trigo, I.F. (2020) The Roles of NDVI and Land Surface Temperature When Using the Vegetation Health Index over Dry Regions. *Global and Planetary Change*, **190**, Article ID: 103198. https://doi.org/10.1016/j.gloplacha.2020.103198

[28] Mo, Y., Xu, Y., Chen, H. and Zhu, S. (2021) A Review of Reconstructing Remotely Sensed Land Surface Temperature under Cloudy Conditions. *Remote Sensing*, **13**, Article 2838. https://doi.org/10.3390/rs13142838

[29] Xie, F. and Fan, H. (2021) Deriving Drought Indices from MODIS Vegetation Indices (NDVI/EVI) and Land Surface Temperature (LST): Is Data Reconstruction Necessary? *International Journal of Applied Earth Observation and Geoinformation*, **101**, Article ID: 102352. https://doi.org/10.1016/j.jag.2021.102352

[30] Ghazaryan, G., König, S., Rezaei, E., Siebert, S. and Dubovyk, O. (2020) Analysis of Drought Impact on Croplands from Global to Regional Scale: A Remote Sensing Approach. *Remote Sensing*, **12**, Article 4030. https://doi.org/10.3390/rs12244030

[31] Halder, S., Roy, M.B. and Roy, P.K. (2022) Modelling Drought Vulnerability Tracts under Changed Climate Scenario Using Fuzzy DEMATEL and GIS Techniques. *Theoretical and Applied Climatology*, **150**, 425-452. https://doi.org/10.1007/s00704-022-04165-7

[32] Bwambale, E., Abagale, F.K. and Anornu, G.K. (2022) Smart Irrigation Monitoring and Control Strategies for Improving Water Use Efficiency in Precision Agriculture: A Review. *Agricultural Water Management*, **260**, Article ID: 107324. https://doi.org/10.1016/j.agwat.2021.107324

[33] Shyam, G.M., Taloor, A.K., Sudhanshu,, Singh, S.K. and Kanga, S. (2021) Sustainable Water Management Using Rainfall-Runoff Modeling: A Geospatial Approach. *Groundwater for Sustainable Development*, **15**, Article ID: 100676. https://doi.org/10.1016/j.gsd.2021.100676

[34] Caceres, C. (2021) A Climate Change Vulnerability Assessment among Small Farmers: A Case Study in Western Honduras. Ph.D. Thesis, The Claremont Graduate University.

[35] Adamides, G., Kalatzis, N., Stylianou, A., Marianos, N., Chatzipapadopoulos, F., Giannakopoulou, M., *et al.* (2020) Smart Farming Techniques for Climate Change

Adaptation in Cyprus. *Atmosphere*, **11**, Article 557. https://doi.org/10.3390/atmos11060557

[36] Simelton, E. and McCampbell, M. (2021) Do Digital Climate Services for Farmers Encourage Resilient Farming Practices? Pinpointing Gaps through the Responsible Research and Innovation Framework. *Agriculture*, **11**, Article 953. https://doi.org/10.3390/agriculture11100953

[37] Wu, B., Ma, Z. and Yan, N. (2020) Agricultural Drought Mitigating Indices Derived from the Changes in Drought Characteristics. *Remote Sensing of Environment*, **244**, Article ID: 111813. https://doi.org/10.1016/j.rse.2020.111813

[38] Tian, Q., Lu, J. and Chen, X. (2022) A Novel Comprehensive Agricultural Drought Index Reflecting Time Lag of Soil Moisture to Meteorology: A Case Study in the Yangtze River Basin, China. *CATENA*, **209**, Article ID: 105804. https://doi.org/10.1016/j.catena.2021.105804

[39] Apori, S.O., Mcmillan, D., Giltrap, M. and Tian, F. (2022) Mapping the Restoration of Degraded Peatland as a Field of Research Area: A Scientometric Review. https://doi.org/10.21203/rs.3.rs-1900121/v2

[40] Kloos, S., Yuan, Y., Castelli, M. and Menzel, A. (2021) Agricultural Drought Detection with MODIS Based Vegetation Health Indices in Southeast Germany. *Remote Sensing*, **13**, Article 3907. https://doi.org/10.3390/rs13193907

[41] Maggi, F., Tang, F.H.M., Black, A.J., Marks, G.B. and McBratney, A. (2021) The Pesticide Health Risk Index—An Application to the World's Countries. *Science of the Total Environment*, **801**, Article ID: 149731. https://doi.org/10.1016/j.scitotenv.2021.149731

[42] Faiz, M.A., Zhang, Y., Ma, N., Baig, F., Naz, F. and Niaz, Y. (2021) Drought Indices: Aggregation Is Necessary or Is It Only the Researcher's Choice? *Water Supply*, **21**, 3987-4002. https://doi.org/10.2166/ws.2021.163

[43] Sa'adi, Z., Yusop, Z., Alias, N.E., Shiru, M.S., Muhammad, M.K.I. and Ramli, M.W.A. (2023) Application of CHIRPS Dataset in the Selection of Rain-Based Indices for Drought Assessments in Johor River Basin, Malaysia. *Science of the Total Environment*, **892**, Article ID: 164471. https://doi.org/10.1016/j.scitotenv.2023.164471

[44] Zaremohzzabieh, Z., Krauss, S.E., D'Silva, J.L., Tiraieyari, N., Ismail, I.A. and Dahalan, D. (2021) Towards Agriculture as Career: Predicting Students' Participation in the Agricultural Sector Using an Extended Model of the Theory of Planned Behavior. *The Journal of Agricultural Education and Extension*, **28**, 67-92. https://doi.org/10.1080/1389224x.2021.1910523

[45] Sharara, A., Shekede, M.D., Gwitira, I., Masocha, M. and Dube, T. (2022) Fine-Scale Multi-Temporal and Spatial Analysis of Agricultural Drought in Agro-Ecological Regions of Zimbabwe. *Geomatics, Natural Hazards and Risk*, **13**, 1342-1365. https://doi.org/10.1080/19475705.2022.2072774

[46] Aduvukha, G.R., Abdel-Rahman, E.M., Sichangi, A.W., Makokha, G.O., Landmann, T., Mudereri, B.T., *et al.* (2021) Cropping Pattern Mapping in an Agro-Natural Heterogeneous Landscape Using Sentinel-2 and Sentinel-1 Satellite Datasets. *Agriculture*, **11**, Article 530. https://doi.org/10.3390/agriculture11060530

[47] D'Allestro, P. and Parente, C. (2015) GIS Application for NDVI Calculation Using Landsat 8 OLI Images. *International Journal of Applied Engineering Research*, **10**, 42099-42102.

[48] Dutta, D., Kundu, A., Patel, N.R., Saha, S.K. and Siddiqui, A.R. (2015) Assessment of Agricultural Drought in Rajasthan (India) Using Remote Sensing Derived Vege-

tation Condition Index (VCI) and Standardized Precipitation Index (SPI). *The Egyptian Journal of Remote Sensing and Space Science*, **18**, 53-63. https://doi.org/10.1016/j.ejrs.2015.03.006

[49] Wang, L., Wang, P., Liang, S., Qi, X., Li, L. and Xu, L. (2019) Monitoring Maize Growth Conditions by Training a BP Neural Network with Remotely Sensed Vegetation Temperature Condition Index and Leaf Area Index. *Computers and Electronics in Agriculture*, **160**, 82-90. https://doi.org/10.1016/j.compag.2019.03.017

[50] Bento, V.A., Gouveia, C.M., DaCamara, C.C. and Trigo, I.F. (2018) A Climatological Assessment of Drought Impact on Vegetation Health Index. *Agricultural and Forest Meteorology*, **259**, 286-295. https://doi.org/10.1016/j.agrformet.2018.05.014

[51] Zang, C.S., Buras, A., Esquivel-Muelbert, A., Jump, A.S., Rigling, A. and Rammig, A. (2019) Standardized Drought Indices in Ecological Research: Why One Size Does Not Fit All. *Global Change Biology*, **26**, 322-324. https://doi.org/10.1111/gcb.14809

[52] Ali, P.J.M., Faraj, R.H., Koya, E., Ali, P.J.M. and Faraj, R.H. (2014) Data Normalization and Standardization: A Technical Report. *Machine Learning Technical Reports*, **1**, 1-6.

[53] McKee, T.B., Doesken, N.J. and Kleist, J. (1993) The Relationship of Drought Frequency and Duration to Time Scales. *Proceedings of the* 8*th Conference on Applied Climatology*, Anaheim, 17-22 January 1993, 179-184.

[54] Abebe, B.A., Grum, B., Degu, A.M. and Goitom, H. (2022) Spatio-Temporal Rainfall Variability and Trend Analysis in the Tekeze-Atbara River Basin, Northwestern Ethiopia. *Meteorological Applications*, **29**, e2059. https://doi.org/10.1002/met.2059

[55] Penalba, O.C. and Rivera, J.A. (2016) Precipitation Response to El Niño/La Niña Events in Southern South America—Emphasis in Regional Drought Occurrences. *Advances in Geosciences*, **42**, 1-14. https://doi.org/10.5194/adgeo-42-1-2016

[56] Vellore, R.K., Kaplan, M.L., Krishnan, R., Lewis, J.M., Sabade, S., Deshpande, N., *et al.* (2015) Monsoon-Extratropical Circulation Interactions in Himalayan Extreme Rainfall. *Climate Dynamics*, **46**, 3517-3546.
https://doi.org/10.1007/s00382-015-2784-x

[57] Miralles, D.G., Brutsaert, W., Dolman, A.J. and Gash, J.H. (2020) On the Use of the Term "Evapotranspiration". *Water Resources Research*, **56**, e2020WR028055.
https://doi.org/10.1029/2020wr028055

[58] Emongor, R.A., Matiri, F.M., Magana, A., Wamaitha, J., Daniel, A.M. and Mulindo, J. (2022) Factors Influencing Adoption of Pigeon Pea and Its Impact on Household Food Security in Machakos County, Kenya. *Asian Journal of Agricultural Extension*, *Economics & Sociology*, **40**, 29-38.
https://doi.org/10.9734/ajaees/2022/v40i430867

[59] Bhattacharya, A. and Bhattacharya, A. (2021) Effect of Soil Water Deficit on Growth and Development of Plants: A Review. In: Bhattacharya, A., Ed., *Soil Water Deficit and Physiological Issues in Plants*, Springer, 393-488.
https://doi.org/10.1007/978-981-33-6276-5_5

[60] Adebara, I.O. (2023) Physiological Response of Legumes to Combined Environmental Stress Factors. In: Mangena, P., Ed., *Advances in Legume Research: Physiological Responses and Genetic Improvement for Stress Resistance*, Bentham Science Publishers, 142-160. https://doi.org/10.2174/9789815165319123020013

[61] Yao, N., Li, Y., Liu, Q., Zhang, S., Chen, X., Ji, Y., *et al.* (2022) Response of Wheat and Maize Growth-Yields to Meteorological and Agricultural Droughts Based on Standardized Precipitation Evapotranspiration Indexes and Soil Moisture Deficit Indexes. *Agricultural Water Management*, **266**, Article ID: 107566.

https://doi.org/10.1016/j.agwat.2022.107566

[62] Dutta Gupta, T., Hassan, G.M., Abdi, A.N., Madurga Lopez, I.M., Liebig, T., Santa Cruz, L.M., Sax, N., Läderach, P. and Pacillo, G. (2023) How Does Climate Exacerbate Root Causes of Conflict in Kenya? Climate Security Pathway Analysis. FACTSHEET 2023/1. CGIAR Focus Climate Security, Rome. https://hdl.handle.net/10568/116458

[63] Holleman, C., Jackson, J., Sánchez, M.V. and Vos, R. (2017) Sowing the Seeds of Peace for Food Security. FAO Agricultural Development Economics Technical Study (FAO) Eng No. 2, p. 95.
https://agris.fao.org/search/en/providers/122621/records/6473b98f13d110e4e7ac2eb2

[64] Kai, K.H., Kijazi, A.L., Osima, S.E., Mtongori, H.I., Makame, M.O., Bakari, H.J., *et al.* (2021) Spatio-Temporal Assessment of the Performance of March to May 2020 Long Rains and Its Socio-Economic Implications in Northern Coast of Tanzania. *Atmospheric and Climate Sciences*, **11**, 767-796.
https://doi.org/10.4236/acs.2021.114045

[65] Liemohn, M.W., Shane, A.D., Azari, A.R., Petersen, A.K., Swiger, B.M. and Mukhopadhyay, A. (2021) RMSE Is Not Enough: Guidelines to Robust Data-Model Comparisons for Magnetospheric Physics. *Journal of Atmospheric and Solar-Terrestrial Physics*, **218**, Article ID: 105624. https://doi.org/10.1016/j.jastp.2021.105624

[66] Modanesi, S., Massari, C., Camici, S., Brocca, L. and Amarnath, G. (2020) Do Satellite Surface Soil Moisture Observations Better Retain Information about Crop-Yield Variability in Drought Conditions? *Water Resources Research*, **56**, e2019WR025855.
https://doi.org/10.1029/2019wr025855

[67] Waseem, M., Jaffry, A.H., Azam, M., Ahmad, I., Abbas, A. and Lee, J. (2022) Spatiotemporal Analysis of Drought and Agriculture Standardized Residual Yield Series Nexuses across Punjab, Pakistan. *Water*, **14**, Article 496.
https://doi.org/10.3390/w14030496

[68] Abbas, S., Nichol, J., Qamer, F. and Xu, J. (2014) Characterization of Drought Development through Remote Sensing: A Case Study in Central Yunnan, China. *Remote Sensing*, **6**, 4998-5018. https://doi.org/10.3390/rs6064998

[69] Zhang, Q., Shi, R., Xu, C., Sun, P., Yu, H. and Zhao, J. (2022) Multisource Data-Based Integrated Drought Monitoring Index: Model Development and Application. *Journal of Hydrology*, **615**, Article ID: 128644.
https://doi.org/10.1016/j.jhydrol.2022.128644